Performance analysis of 20 Gb/s RZ-DPSK non-slope matched transoceanic submarine links

Brendan Slater,[1] Sonia Boscolo,[1*] Terence Broderick,[1] Sergei K. Turitsyn,[1], Ronald Freund,[2] Lutz Molle,[2] Christoph Caspar,[2] Jörg Schwartz,[3] and Stuart Barnes[3]

[1]*Photonics Research Group, School of Engineering and Applied Science, Aston University, Birmingham B4 7ET, United Kingdom*

[2]*Fraunhofer-Institute for Telecommunications, Heinrich-Hertz-Institut, Einsteinufer 37, 10587 Berlin, Germany*

[3]*Azea Networks Ltd., Bates House, Harold Wood, Romford RM3 0SD, United Kingdom*

[*] *Corresponding author: s.a.boscolo@aston.ac.uk*

Abstract: Direct computation of the bit-error rate (BER) and laboratory experiments are used to assess the performance of a non-slope matched transoceanic submarine transmission link operating at 20 Gb/s channel rate and employing return-to-zero differential-phase shift keying (RZ-DPSK) signal modulation. Using this system as an example, we compare the accuracies of the existing theoretical approaches to the BER estimation for the RZ-DPSK format.

OCIS codes: (060.2330) Fiber optics communications; (060.2360) Fiber optics links and subsystems.

References and links

1. L. Becouarn, G. Vareille, P. Pecci, and J. F. Marcerou, "3 Tbit/s transmission (301 DPSK channels at 10.709 Gb/s) over 10 270 km with a record efficiency of 0.65 bit/s/Hz," in *Proceedings of 29th European Conference on Optical Communication*, Rimini, Italy, Sept. 2003, postdeadline paper Th4.3.2.
2. A. H. Gnauck, G. Raybon, S. Chandrasekhar, J. Leuthold, C. Doerr, L. Stulz, A. Agarwal, S. Banerjee, D. Grosz, S. Hunsche, A. Kung, A. Marhelyuk, D. Maywar, M. Movassaghi, X. Liu, C. Xu, X. Wei, and D. M. Gill, "2.5 Tb/s (64×42.7 Gb/s) transmission over 40×100 km NZDSF using RZ-DPSK format and all-Raman-amplified spans," in *Optical Fiber Communications Conference*, OSA Technical Digest Series (Optical Society of America, 2002), postdeadline paper FC2.
3. A. H. Gnauck and P. J. Winzer, "Optical phase-shift-keyed transmission," J. Lightwave Technol. **23,** 115–130 (2005).
4. J.-X. Cai, D. G. Foursa, L. Liu, C. R. Davidson, Y. Cai, W. W. Patterson, A. J. Lucero, B. Bakhshi, G. Mohs, P. C. Corbett, V. Gupta, W. Anderson, M. Vaa, G. Domagala, M. Mazurczyk, H. Li, S. Jiang, M. Nissov, A. N. Pilipetskii, and N. S. Bergano, "RZ-DPSK field trial over 13 100 km of installed non-slope-matched submarine fibers," J. Lightwave Technol. **23,** 95–103 (2005).
5. J. -X. Cai, C. R. Davidson, M. Nissov, H. Li, W. Anderson, Y. Cai, L. Liu, A. N. Pilipetskii, D. G. Foursa, W. W. Patterson, P. C. Corbett, A. J. Lucero, and N. S. Bergano, "Transmission of 40 Gb/s WDM signals over 6,250 km of conventional NZ-DSF with >4 dB FEC margin," in *Optical Fiber Communication Conference and Exposition and The National Fiber Optic Engineers Conference*, Technical Digest (CD) (Optical Society of America, 2005), paper PDP26. .
6. J. -X. Cai, M. Nissov, H. Li, C. R. Davidson, W. Anderson, L. Liu, D. G. Foursa, A. N. Pilipetskii, and N. S. Bergano, "Experimental comparison of 40 Gb/s RZ-, CSRZ-, and NRZ-DPSK modulation formats over non

#79809 - $15.00 USD Received 7 Feb 2007; revised 8 May 2007; accepted 9 May 2007; published 17 Aug 2007

slope-matched fibres," in *Proceedings of 31st European Conference on Optical Communication*, Glasgow, Scotland, Sept. 2005, paper Th1.2.2.
7. J. -X. Cai, M. Nissov, W. Anderson, M. Vaa, C. R. Davidson, D. G. Foursa, L. Liu, Y. Cai, A. J. Lucero, W. W. Patterson, P. C. Corbett, A. N. Pilipetskii, and N. S. Bergano, "Long-haul 40 Gb/s RZ-DPSK transmission with long repeater spacing," in *Optical Fiber Communication Conference and Exposition and The National Fiber Optic Engineers Conference*, Technical Digest (CD) (Optical Society of America, 2005), paper OFD3.
8. R. Freund, L. Molle, C. Caspar, J. Schwartz, S. Webb, and S. Barnes, "Mixed bitrate and modulation format upgrades of non-slope matched submarine links," in *Proceedings of 32nd European Conference on Optical Communication*, Cannes, France, Sept. 2006, paper Th1.6.5.
9. A. N. Pilipetskii, "Propagation effects at high bit rates," in O*ptical Fiber Communication Conference and Exposition and The National Fiber Optic Engineers Conference*, Technical Digest (CD) (Optical Society of America, 2006), paper OWJ7.
10. N. S. Bergano, F. W. Kerfoot, and C. R. Davidson, "Margin measurements in optical amplifier system," IEEE Photon. Technol. Lett. **5,** 304–306 (1993).
11. C. Xu, X. Liu, and X. Wei, "Differential phase-shift keying for high spectral efficiency optical transmissions," IEEE J. Sel. Top. Quantum Electron. **10,** 281–293 (2004).
12. C. C. Hiew, F. M. Abbou, H. T. Chuah, S. P. Majumder, and A. A. R. Hairul, "BER estimation of optical WDM RZ-DPSK systems through the differential phase *Q*," IEEE Photon. Technol. Lett. **16,** 2619–2621 (2004).
13. P. A. Humblet and M. Azizoglu, "On the bit error rate of lightwave systems with optical amplifiers," IEEE Photon. Technol. Lett. **15,** 617–619 (2003).
14. G. Bosco and P. Poggiolini, "On the Q factor inaccuracy in the performance analysis of optical direct-detection DPSK systems," IEEE Photon. Technol. Lett. **16,** 665–667 (2004).

1. Introduction

New submarine fiber transmission solutions are required to meet transoceanic traffic needs over the next few years. With existing optical fiber undersea networks being mostly operated at 10 Gb/s channel rate using conventional optical signal amplitude-shift keying (ASK) modulation, an obvious question that emerges in the study of their upgrades is the potential for deploying higher bit rates in conjunction with advanced modulation formats. Direct-detection differential phase-shift keying (DPSK) modulation has recently attracted much attention with regard to high-capacity long-haul lightwave transmissions [1, 2, 3], due to the theoretical limit of 3-dB improvement in receiver sensitivity compared to IM formats and enhanced tolerance to nonlinear impairments. The application of DPSK to legacy undersea systems using the conventional non-slope matched dispersion-shifted fibers has already been demonstrated at both 10 Gb/s [4] and 40 Gb/s [5, 6] channel rates. However, recently a side-by-side comparison of 10 Gb/s and 40 Gb/s return-to-zero (RZ) DPSK using the same spectral efficiency over transoceanic distances showed a lower net bit-error rate (BER) margin for 40 Gb/s [7]. Most recently, 20 Gb/s RZ-DPSK was indicated as a strong candidate for upgrading non-slope matched undersea transmission links, by offering the potential for similar performance as 10 Gb/s RZ-ASK at twice the spectral efficiency, and higher performance than 40 Gb/s RZ-DPSK at the same spectral efficiency [8]. Note that a variety of new transmission regimes similar to that in high-bit-rate systems can be applied even in existing systems operating at lower bit rate. For instance, as it was pointed out in [9], a pseudo-linear, bit-overlapping transmission regime that is typically attributed to 40 Gb/s systems can be advantageously applied at 10 Gb/s rates using short carrier pulses and RZ-DPSK format. We would like to stress that by varying the pulse duty cycle at 20 Gb/s channel rate it is possible to realise quite different transmission regimes, ranging from a pseudo-linear regime to a dispersion-managed soliton-like one. Therefore, an optimal choice of the duty cycle in 20 Gb/s ultra-long-haul systems is an interesting and open research problem.

The major goal of this paper is to assess the performance of a typical non-slope matched transoceanic submarine transmission link using 20 Gb/s channel rate and RZ-DPSK modulation with different duty cycles. We also discuss an important issue of system performance evaluation and compare the predictions of the system performance based on different available *Q*-factor models for the RZ-DPSK format [10, 11, 12] to the actual BER computed via direct error

#79809 - $15.00 USD Received 7 Feb 2007; revised 8 May 2007; accepted 9 May 2007; published 17 Aug 2007

counting. The numerical results are compared with laboratory experiments.

2. System description and numerical modeling

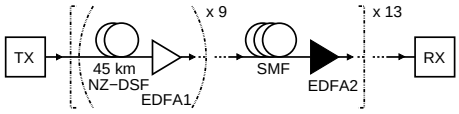

Fig. 1. Setup of the transmission system.

The transmission link used in our analysis is depicted in Fig. 1. The unit cell of the system is composed of nine sections of non-zero dispersion-shifted fiber (NZ-DSF) of length 45 km each, followed by a section of standard monomode fiber (SMF). The NZ-DSF has a dispersion of $D = -3\,\mathrm{ps}/(\mathrm{nm\,km})$, a dispersion slope of $S = 0.09\,\mathrm{ps}/(\mathrm{nm^2\,km})$, an attenuation of $\alpha = 0.2\,\mathrm{dB/km}$, and an effective area of $A_{\mathrm{eff}} = 54\,\mu\mathrm{m}^2$. The parameters of the SMF are: $D = 16\,\mathrm{ps}/(\mathrm{nm\,km})$, $S = 0.057\,\mathrm{ps}/(\mathrm{nm^2\,km})$, $\alpha = 0.2\,\mathrm{dB/km}$, and $A_{\mathrm{eff}} = 80\,\mu\mathrm{m}^2$. The D, α, and A_{eff} values are given at 1550 nm. The nonlinear Kerr coefficient is $2.35 \times 10^{-20}\,\mathrm{m}^2/\mathrm{W}$. The accumulated dispersion of the NZ-DSF is completely compensated for by the SMF. Erbium-doped fiber amplifiers (EDFAs) 1 and 2 with a noise figure of 4.5 dB are used at the end of each NZ-DSF section and the SMF span, respectively, to compensate for the energy losses in the fibers. The unit cell of the system is repeated thirteen times to yield a total transmission length of approximately 6300 km. 20 Gb/s RZ-DPSK random bit sequences formed with Gaussian pulses are transmitted over the line. At the receiver, the signal is filtered using a Gaussian optical bandpass filter (OBPF)/demultiplexer (DEMUX), detected using a balanced Mach-Zehnder delay interferometer (DI), and then filtered electrically by a third-order Butterworth filter with a cutoff frequency equal to the bit rate.

Since direct computation of very low BERs can be difficult, indirect statistical and numerical methods for system performance evaluation are imperative. The Q-factor, which is closely related to the error probability, is a widely used tool to estimate the performance of optical transmission systems because it is relatively easy to evaluate, thus preventing the need for time-consuming direct counting of errors. For IM systems, the Gaussian approximated Q-factor of the received electrical signal [10] is commonly used to estimate the BER because it provides a relatively good estimate, even though the actual noise distribution is not exactly Gaussian [13]. It is defined as $Q_{\mathrm{el}} = |\mu_1 - \mu_0|/(\sigma_1 + \sigma_0)$ with $\mathrm{BER}(Q_{\mathrm{el}}) = (1/2)\mathrm{erfc}(Q_{\mathrm{el}}/\sqrt{2})$, where $\mu_{1,0}$ and $\sigma_{1,0}$ are the mean and standard deviation of the decision variable when a logical "one" or "zero" are transmitted, and erfc is the complementary error function. However, it was stressed in [14, 11] that a direct transfer of this method into DPSK systems can be unreliable. This discrepancy is attributed to the fundamentally non-Gaussian nature of the noise distribution in the output signal of the DPSK balanced receiver. It was suggested [11] that a more accurate prediction of the BER in DPSK modeling in a linear channel can be obtained by evaluating the variance of the field amplitude $|f_n|$ before the DI, and an alternative amplitude Q was introduced, defined as $Q_A = \langle |f_n| \rangle / \sigma_{|f_n|}$. Another alternative Q-parameter, the differential phase Q, was also introduced to estimate the BER in the nonlinear regime when the DPSK transmission performance is limited by phase noise. It is defined as $Q_{\Delta\phi} = \pi/(\sigma_{\Delta\phi,0} + \sigma_{\Delta\phi,\pi})$, where $\sigma_{\Delta\phi,0}$ and $\sigma_{\Delta\phi,\pi}$ are the standard deviations of the optical differential phase (phase difference between two sampling points separated by one bit period mapped from $[-\pi/2, 3\pi/2]$) of the received signal on the zero and π rails, respectively. The BER can be computed from Q_A and $Q_{\Delta\phi}$ using the relations $\mathrm{BER}(Q_A) = (1/2)\exp(-Q_A^2/2)$ and $\mathrm{BER}(Q_{\Delta\phi}) = \mathrm{erfc}(Q_{\Delta\phi}/\sqrt{2})$ [11], which are calculated using the Gaussian approximation of the field amplitude noise and the noise at the

#79809 - $15.00 USD Received 7 Feb 2007; revised 8 May 2007; accepted 9 May 2007; published 17 Aug 2007

center of each rail of the differential phase eye diagram, respectively. To improve the accuracy of the differential phase Q, a correction to the Gaussian approximation for the phase noise was proposed in [12], which yielded a modified differential phase Q equal to $Q_{\Delta\phi,\mathrm{mod}} = 0.87Q_{\Delta\phi}$.

3. Numerical and experimental results

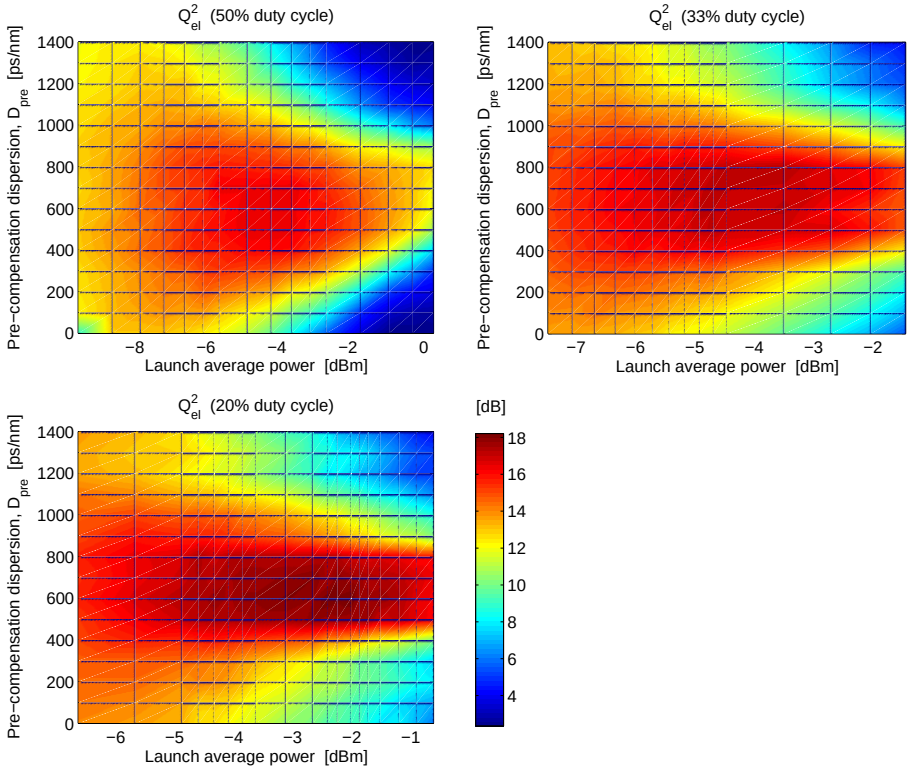

Fig. 2. Electrical Q^2-factor versus launch signal average power and pre-compensation dispersion.

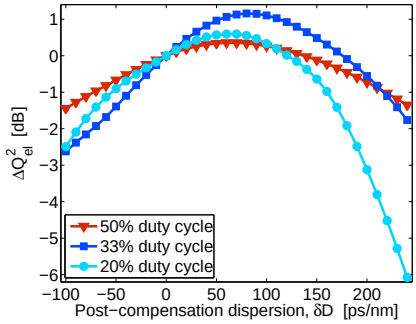

Fig. 3. Electrical Q^2-factor variation with the fine-tuning post-compensation dispersion.

First, we optimize the system performance versus the pre- and post-compensation disper-

#79809 - $15.00 USD Received 7 Feb 2007; revised 8 May 2007; accepted 9 May 2007; published 17 Aug 2007

sions and the launch signal power for different duty cycles of the input pulses through single-channel transmission simulations. We use the electrical Q-factor as an indicator of the system performance. The Q-factor is calculated at the end of the unit cell of the link, and averaged over a number of 1024-bit pattern runs. A (not optimized) 3-dB bandwidth of 45 GHz is used for the receiver OBPF. Figure 2 shows the Q^2-factor at the output of the transmission link as a function of the average power of the input signal and the pre-compensation dispersion, D_{pre}, for the pulse duty cycles of 50%, 33%, and 20%. Here, the post-compensation dispersion, $D_{\text{post,large-scale}}$, is selected such that $D_{\text{post,large-scale}} = -D_{\text{pre}}$ (at zero line average dispersion), i.e., a 50/50 pre/post-compensation ratio is used. It can be seen that the optimum pre-compensation and average power vary from approximately (500 ps/nm, -4.3 dBm) for the 50% duty cycle, to approximately (800 ps/nm, -3.6 dBm) for the 33% duty cycle, and to (600 ps/nm, -2.1 dBm) for the shortest duty cycle, while there are sufficiently large power margins within the dispersion range 500 ps/nm to 800 ps/nm for all duty cycles. It is also seen that the system performance is improved by use of narrow pulses, as expected in the case of single-channel transmission [9]. The optimum system performance is ultimately assessed through fine tuning of the post-compensation dispersion by addition of a dispersion amount δD to the large-scale post-compensation, such that the total post-compensation dispersion is $D_{\text{post,tot}} = D_{\text{post,large-scale}} + \delta D$. We quantify the performance variation with tuning of δD by the difference ΔQ^2_{el} between the electrical Q^2-factor at a given δD and the Q^2-value at zero δD. The results are reported in Fig. 3 as a function of δD for the three duty cycles studied. It can be seen that the system performance is optimized by a positive δD between 50 ps/nm and 100 ps/nm for all duty cycles. The largest duty cycle is the most tolerant to variations in δD, but its performance improvement at the optimum δD is the smallest. The 33% duty cycle exhibits the largest Q^2-factor improvement of more than 1 dB at the optimum δD.

Based on these settings, we compare the accuracy of the electrical, amplitude, and differential phase Q-factor models versus the actual BER obtained from direct error counting in single-channel transmission simulations. Direct computation is limited to BERs of 10^{-4} or higher so that good error statistics can be obtained within a reasonable amount of computation time. For this purpose, we transmit sequences of 16384 bits over larger distances than the total length of the transmission link. The optimum power and D_{pre} ($D_{\text{post,large-scale}}$) suggested by the results in Fig. 2 are used, and δD is optimized at each distance where the BER is computed by use of Q_{el}. Figure 4 shows the BER as a function of the transmission distance. It is seen that Q_{el} underestimates the actual BER with a similar discrepancy for all pulse widths. The significant BER underestimation by Q_A at any pulse width is an indication that the transmission regime is nonlinear [11]. $Q_{\Delta\phi}$ slightly overestimates the BER for the 50% duty cycle, and it underestimates the BER for the shorter duty cycles with a discrepancy that increases with decreasing pulse width. Consequently, the amount of BER overestimation by $Q_{\Delta\phi,\text{mod}}$ reduces with decreasing pulse width, which results in a rather correct estimate for the shortest duty cycle. The magnitude of the discrepancies of the various BER estimates to the actual BER indicates that $Q_{\Delta\phi}$ is the most reliable performance indicator for the 50% duty cycle and $Q_{\Delta\phi,\text{mod}}$ offers the highest accuracy for the 20% duty cycle, whereas for the 33% duty cycle the two phase Q-factors compete with one another at giving the most reliable performance prediction. It can also be seen from Fig. 4 that the shorter duty cycles achieve the higher BER margin. Indeed, supposing an extension of the directly computed BER curves to the region of short distances with either BER$(Q_{\Delta\phi})$ or BER$(Q_{\Delta\phi,\text{mod}})$ as a reference curve, a BER of 10^{-9} would relate to a transmission distance of approximately 6000 km for the 50% duty cycle, and 8000 km for the 33% and 20% duty cycles.

An explanation for the degree of accuracy of the BER estimates through the different Q models can be found by looking at the probability density functions (PDFs) for the relevant qantities

#79809 - $15.00 USD Received 7 Feb 2007; revised 8 May 2007; accepted 9 May 2007; published 17 Aug 2007

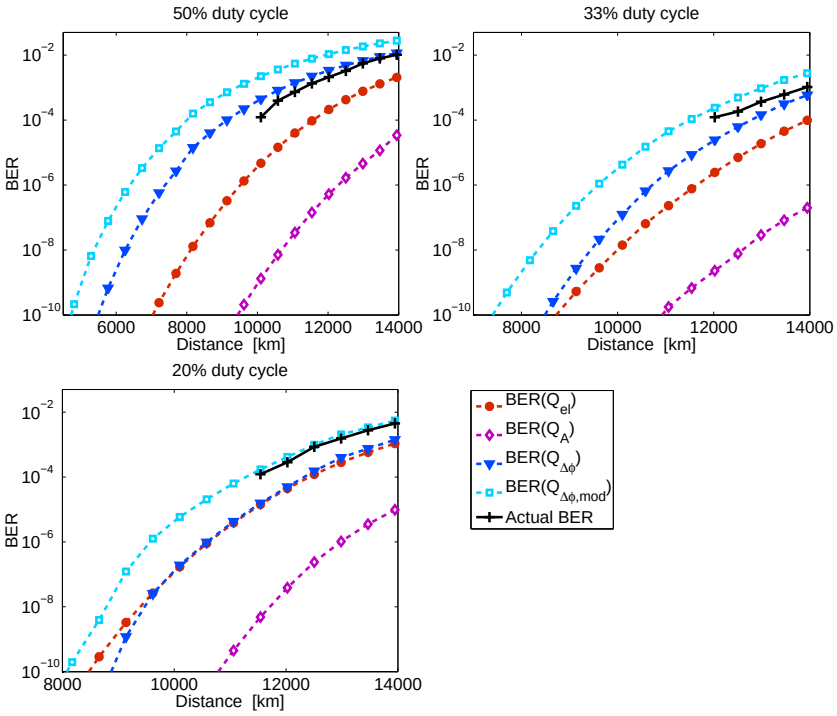

Fig. 4. Theoretical BERs and directly computed BER versus distance for 20 Gb/s single-channel RZ-DPSK transmission.

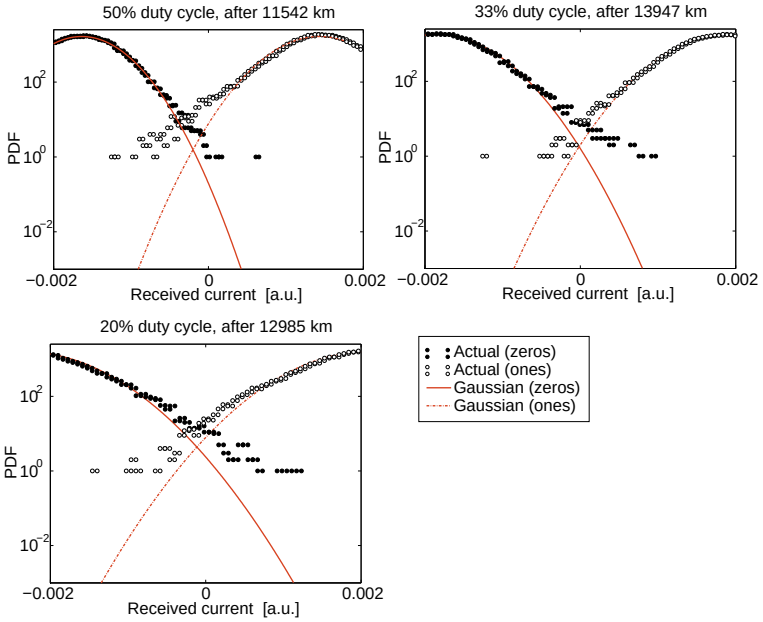

Fig. 5. Distributions of received current: actual distributions and approximations.

#79809 - $15.00 USD Received 7 Feb 2007; revised 8 May 2007; accepted 9 May 2007; published 17 Aug 2007

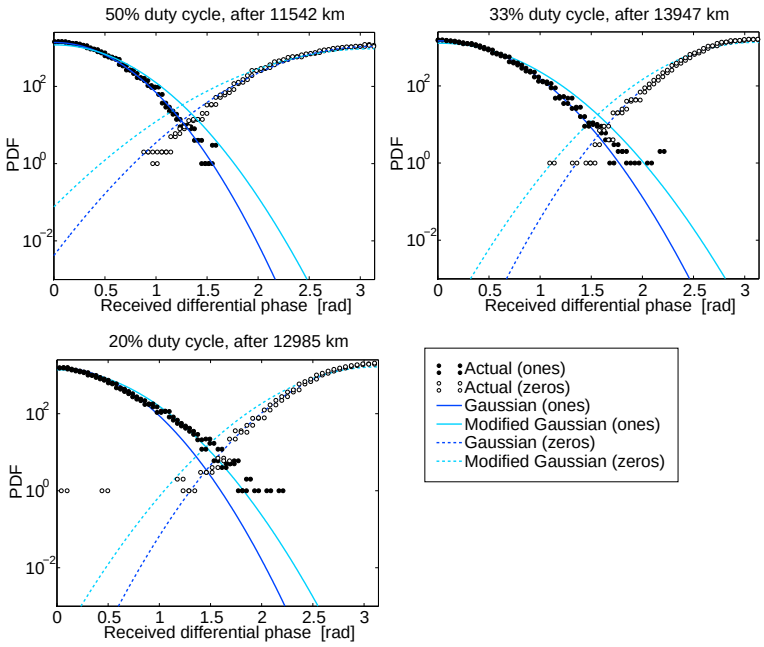

Fig. 6. Distributions of received differential phase: actual distributions and approximations.

of the received signal. Figures 5 and 6 shows the PDFs of the received current and differential phase for the "ones" and the "zeros" obtained at similar values of BER (approximately 10^{-3}) for the three duty cycles. The deviations of the actual distributions from the approximations (Gaussian or modified Gaussian) underlying the pertinent Q models consistently explain the results shown in Fig. 4. In particular, a closer inspection of the PDFs' tails reveals that the kurtosis of the actual distributions is in general larger than the value of three of the corresponding Gaussian distributions. Note that the modified Gaussian approximations for the PDFs of the received differential phase have a kurtosis of approximately 1.72 as they correspond to a correction factor of 1.15 multiplied to $\sigma_{\Delta\phi,0}$ and $\sigma_{\Delta\phi,\pi}$ in the respective Gaussian distributions [12]. It is also seen that the "non-gaussianicity" of the tails of the actual distributions increases with decreasing pulse width.

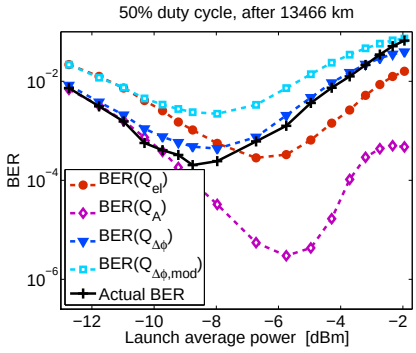

Fig. 7. Theoretical BERs and directly computed BER versus launch signal average power.

#79809 - $15.00 USD Received 7 Feb 2007; revised 8 May 2007; accepted 9 May 2007; published 17 Aug 2007

The dependence of the BER estimates obtained from the different Qs on the signal power is illustrated in Fig. 7, where the theoretical BERs are compared to the directly computed BER over a range of launch signal average powers with 50% duty cycle pulses as an example, at a BER of approximately 10^{-4} for the optimum case in the figure. An optical signal-to-noise ratio of about 9 dB/nm is recorded after the considered transmission distance of 13466 km at approximately -10 dBm launch average power. It can be seen from Fig. 7 that BER$(Q_{\Delta\phi})$ [11] is consistently the most accurate estimate of the actual BER at any power level for this duty cycle, whereas Q_{el} overestimates (underestimates) the BER at the lower powers (higher powers). It is also seen that the BER curve calculated from $Q_{\Delta\phi}$ (or equivalently $Q_{\Delta\phi,\mathrm{mod}}$) [12] more closely mimics that of the actual BER. This is in agreement with the predictions of [11] and [12].

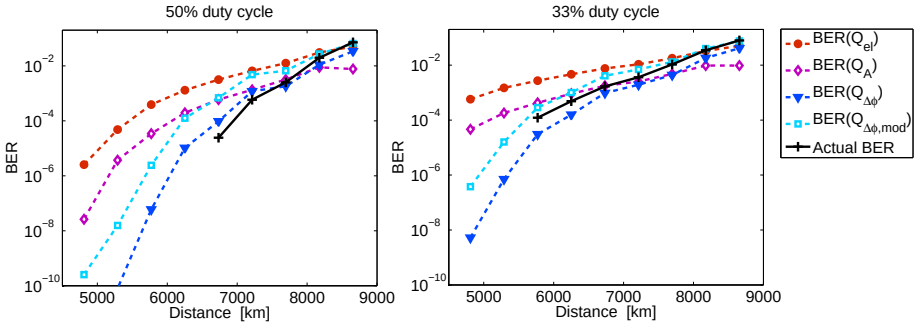

Fig. 8. Theoretical BERs and directly computed BER versus distance for 50 GHz-spaced 20 Gb/s WDM RZ-DPSK transmission.

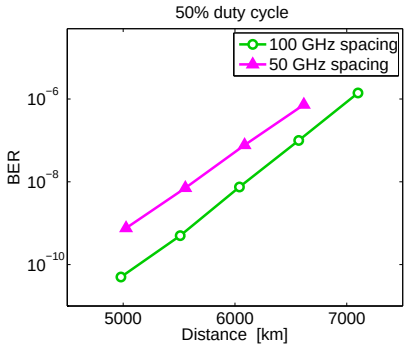

Fig. 9. Measured BER versus distance for 20 Gb/s WDM RZ-DPSK transmission with 50% duty cycle.

Next, we analyze the BER performance of wavelength-division multiplexed (WDM) transmission at 50 GHz channel separation (0.4 bit/(s Hz) spectral efficiency). We transmit three wavelength channels (1552.8 nm to 1553.6 nm), each modeled by a 16384-bit sequence. Figure 8 shows the theoretical BERs and actual BER of the channel centred at 1553.2 nm versus the transmission distance for the 50% and 33% pulse duty cycles. The optimum launch power and pre-compensation dispersion (large-scale post-compensation dispersion) suggested by the single-channel results in Fig. 2 are used for all channels, and the fine-tuning post-compensation dispersion is optimized at each distance where the BER is calculated. The 3-dB bandwidth of

#79809 - $15.00 USD Received 7 Feb 2007; revised 8 May 2007; accepted 9 May 2007; published 17 Aug 2007

the DEMUX is optimized to 30 GHz for the 50% duty cycle and 20 GHz for the 33% duty cycle through back-to-back simulations, and the results are averaged over a number of runs. It can be seen that either $Q_{\Delta\phi}$ or $Q_{\Delta\phi,\mathrm{mod}}$ is the best performance indicator in terms of a trade-off between accuracy in the predictions and mimicking of the actual BER curves. It is also seen that the BER margin is improved by the use of large pulses. Indeed, for instance, at a transmission distance of 6000 km the directly computed BER would be of the order of 10^{-7} for the 50% duty cycle if the BER curve was extended to the short distance region, whereas at the same distance the BER is 2.5×10^{-4} for the 33% duty cycle. Note that linear crosstalk is likely to account for the poorer system performance when using short pulses in the WDM environment considered in this paper, where signal multiplexing is accomplished without optical filtering. The results for the 50% duty cycle pulses show that error-free 20 Gb/s RZ-DPSK transmission at 50 GHz channel separation is feasable beyond the design length of typical installed submarine links with no need for in-band slope compensation of chromatic dispersion, which confirms the experimental observations in [8]. The WDM system performance assessed through numerical simulations is compared to the experimental results. Figure 9 shows the measured BER as a function of the transmission distance at the spectral efficiencies of $0.2\,\mathrm{bit/(s\,Hz)}$ and $0.4\,\mathrm{bit/(s\,Hz)}$. The transmission link is implemented as a re-circulating fiber twin-loop where one orbit consists of 9×45.7 km-NZ-DSF spans and 1×73 km-SMF span (see Ref. [8] for details). Four EDFAs are used in the setup to compensate for fiber loss and insertion loss of the loop components. In addition, the loop configuration contains two fiber Bragg grating-based notch filters to suppress amplified spontaneous emission noise peaks. The output power of the EDFAs is adjusted to about 9 dBm total launch power into both the NZ-DSF section and the SMF section. The launched signal is generated by a WDM transmitter generating sixteen co-polarized channels (1546.12 nm to 1558.17 nm) and for pseudorandom binary sequences of $2^{23} - 1$. Three RZ-DPSK channels plus thirteen continuous-wave wavelengths are used for the measurements at 50 GHz channel spacing, and the results are shown for a 1553.33 nm centred channel. The duty cycle of the pulses is 50%. The differential delay of the Mach-Zehnder interferometer-based optical demodulator at the receiver is 40.3 ps. The comparison of the curve relative to 50 GHz channel spacing with the numerical results suggests a fair agreement at the considered distances. Precise modeling of the experimental scenario and accurate comparison between theoretical and experimental results will be addressed in a future work.

4. Conclusion

We have assessed the performance of a typical non-slope matched transoceanic submarine link using 20Gb/s channel rate and RZ-DPSK modulation. First, optimization of the pre- and post-compensation dispersions, and launch signal power has been performed for different pulse duty cycles. Next, through comparison with direct error counting, we have demonstrated the limitations of the available numerical approaches to the BER estimation for RZ-DPSK. The numerical results have been confirmed by experiments, and indicate that 20 Gb/s RZ-DPSK transmission is a feasible technique for the upgrade of existing submarine links.

Acknowledgments

S. Boscolo gratefully acknowledges the Leverhulme Trust for supporting her work through an Early Career Fellowship.

#79809 - $15.00 USD Received 7 Feb 2007; revised 8 May 2007; accepted 9 May 2007; published 17 Aug 2007